

ISSN2218-2004 www.mdpi.com/journal/atoms

Review

# Emission of $\beta^+$ Particles Via Internal Pair Production in the $0^+-0^+$ Transition of $^{90}$ Zr: Historical Background and Current Applications in Nuclear Medicine Imaging

# Marco D'Arienzo 1,2

- <sup>1</sup> Istituto Nazionale di Metrologia delle Radiazioni Ionizzanti, ENEA, Centro Ricerche Casaccia, Rome, Italy/ Via Anguillarese 201, 00123 Roma; E-Mail: marco.darienzo@enea.it (M.D.); Tel.: +39-06-3048-4118; Fax: +39-06-3048-3558
- <sup>2</sup> Department of Human Anatomy, Histology, Forensic Medicine and Orthopedics, Sapienza University of Rome, Via Borelli 50, 00161 Rome, Italy

Received: 23 January 2013; in revised form: 14 February 2013 / Accepted: 26 February 2013 / Published: 8 March 2013

**Abstract:**  $^{90}$ Y is traditionally considered as a pure  $\beta^-$  emitter. However, the decay of this radionuclide has a minor branch to the  $0^+$  first excited state of  $^{90}$ Zr at 1.76 MeV, that is followed by a  $\beta^+/\beta^-$  emission. This internal pair production has been largely studied in the past because it is generated by a rare electric monopole transition (E0) between the states  $0^+/0^+$  of  $^{90}$ Zr. The positronic emission has been recently exploited for nuclear medicine applications, i.e. positron emission tomography (PET) acquisitions of  $^{90}$ Y-labelled radiopharmaceuticals, widely used as therapeutic agents in internal radiation therapy. To date, this topic is gaining increasing interest in the radiation dosimetry community, as the possibility of detecting  $\beta^+$  emissions from  $^{90}$ Y by PET scanners may pave the way for an accurate patient-specific dosimetry. This could lead to an explosion in scientific production in this field. In the present paper the historical background behind the study of the internal pair production of the  $0^+/0^+$  transition of  $^{90}$ Zr is presented along with most up to date measured branch ratio values. An overview of most recent studies that exploit  $\beta^+$  particles emitted from  $^{90}$ Y for PET acquisitions is also provided.

**Keywords:** Internal pair production; monopole transition;  $^{90}$ Y decay; positron emission tomography.

### 1. Introduction

 $^{90}$ Y is one of the radionuclides most widely used in nuclear medicine therapeutic applications. Thanks to its long β particle range,  $^{90}$ Y allows a uniform irradiation of large tumors commonly expressing heterogeneous perfusion and hypoxia. The average energy of β emissions from  $^{90}$ Y is 0.9367 MeV, with a mean tissue penetration of 2.5 mm and a maximum of 11 mm. However, although  $^{90}$ Y has been traditionally considered as a pure β emitter, the decay of this radionuclide has a minor branch to the  $^{0+}$  first excited state of stable  $^{90}$ Zr at 1.76 MeV, which is followed by a  $^{0+}$ β emission with an extremely small branching ratio. For decades this transition was not exploited in nuclear medicine. Recently, it was proposed to use this pair production in molecular radiation therapy in order to assess  $^{90}$ Y biodistribution by positron emission tomography (PET) acquisitions, especially in regions that may show a high  $^{90}$ Y concentration during internal radiotherapy procedures. This is because PET imaging allows high-resolution images to be obtained if compared to bremsstrahlung SPECT, alternatively used to monitor  $^{90}$ Y biodistribution following therapeutic administration of  $^{90}$ Y-labelled radiopharmaceuticals.

In the last few years, there has been growing interest in liver radioembolization with <sup>90</sup>Y microspheres for the treatment of unresectable hepatocellular carcinoma and liver metastases. It consists of <sup>90</sup>Y embedded into non-biodegradable glass or resin microspheres selectively administered by intra-arterial hepatic injection giving high doses of radiation to the tumor and sparing the liver parenchyma. With this technique, a high activity of <sup>90</sup>Y is likely to be accumulated in a small region of the body (i.e. the liver), thus allowing a sufficient number of positrons to be detected by most commercial PET scanners.

In the present paper the historical background behind the study of the internal pair production of the  $0^+/0^+$  transition of  $^{90}$ Zr is presented along with the most recent branch ratio measurements. A precise knowledge of the branch ratio is important for an accurate quantification of  $^{90}$ Y accumulated inside the target region. An overview of most recent studies that exploit  $\beta^+$  particles emitted from  $^{90}$ Y for PET acquisitions is also provided.

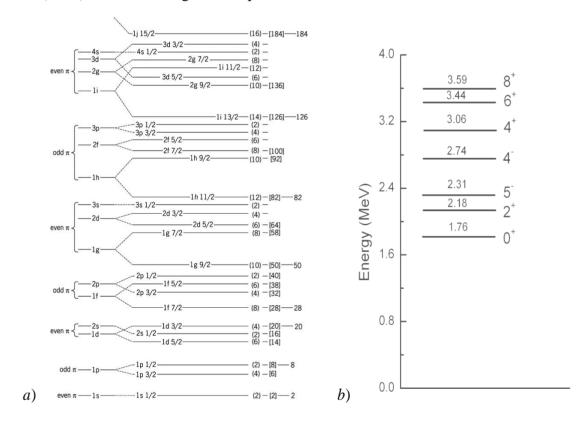
# 2. Internal Pair Production Following the $0^+$ – $0^+$ Transition of $^{90}$ Zr

In the past there has been a great interest in so-called electric monopole transitions (E0) in certain nuclei. This may occur when there is no angular momentum change between initial and final nuclear states and no parity change (in particular, electromagnetic transition between states with J=0). For spin-zero to spin-zero transitions, single gamma emission is strictly forbidden, hence three alternative processes may occur: a) transitions give rise to transfer of radiation energy to an atomic electron in the orbital cloud by internal conversion b) if the energy of the process is greater than  $2m_e c^2$  (1.022 MeV, where  $m_e$  is the mass of the electron), transition can occur via electron-positron internal pair creation. c) two-photon emission, which is generally negligibly small.

The electric monopole transition takes place entirely in the nuclear volume, corresponding classically to a radially oscillating spherical charge distribution that does not give rise to a time-varying field outside the charged region. This may be visualized as a "breathing" mode without change of shape, that is only possible in a compressible nucleus. Past literature studies focused on a

number of nuclei that undergo electric monopole transition. Among these, <sup>16</sup>O, <sup>40</sup>Ca, <sup>72</sup>Ge, <sup>90</sup>Zr have been studied. The importance behind these transitions lies in the fact that the analysis of the small branch ratio associated with two-photon decay provided useful information on the nuclear structure. A surprising result of these researches was that the angular correlation between the two gamma rays was asymmetric about 90°. This was interpreted as arising from interference between the 2E1 and the 2M1 contributions to the transitions which were found to be of comparable strength [1].

**Figure 1**. a) Approximate level pattern for protons derived from the shell model. The spin-orbit coupling is adjusted in such a way that the empirical level sequence is represented. Round brackets (2), (4) *etc*. and square brackets [2], [6], *etc*. denote the level degeneracies and the total occupation number, respectively. b) Experimental energy levels of  $^{90}$ Zr (MeV). The total energies are reported.



In particular, a number of past literature studies were dedicated to the analysis of the electric monopole transition (E0) occurring during the decay of  $^{90}$ Y nucleus to the fundamental level of  $^{90}$ Zr. Figure 1a shows the approximate level pattern for protons derived from the shell model of  $^{90}$ Zr, while Figure 1b) shows the associated low-lying excitations.  $^{90}$ Zr has 40 protons and 50 neutrons. 50 neutrons form a close shell, filling up to  $1g_{9/2}$ . 28 of 40 protons fill first four shells, while the remaining 12 fill  $2p_{3/2}$ ,  $1f_{5/2}$  and  $2p_{1/2}$ . If one of the protons in  $2p_{1/2}$  is excited to  $1g_{9/2}$ , the remaining proton in  $2p_{1/2}$  and the proton in  $1g_{9/2}$  can form states with odd parity and J=4 and 5. There are indeed  $4^{-1}$  and  $5^{-1}$  states. State 5 is lower presumably because two protons are closer in space by lining up the orbital angular momenta. If both protons are excited from  $2p_{1/2}$  to  $1g_{9/2}$ , it could give J=0,1,2,3,4,5,6,7,8,9. Nevertheless, the anti-symmetry of the wave function allows only states with

J = 0, 2, 4, 6, 8. They should all have even parity. Indeed,  $0^+$ ,  $2^+$ ,  $4^+$ ,  $6^+$ ,  $8^+$  are observed in this order (Figure 1b).

The radioactive decay of  $^{90}$ Y nucleus by beta emission to the fundamental level of  $^{90}$ Zr with a half-life of 64 hours has been widely studied in the past. However, in 1955 in a letter to the editor of the *Physical Review*, Ford predicted an excited state (0<sup>+</sup> state) of  $^{90}$ Zr [2]. For the aforementioned reasons, the evidence of the 0<sup>+</sup> state of  $^{90}$ Zr could be proved with the detection of positrons emitted from a  $^{90}$ Y source beta decaying to  $^{90}$ Zr. As a matter of fact, the predicted state was discovered by Johnson *et al.* at the same laboratory in the same period and was described in a letter to the editor of the same journal issue [3]. The authors discovered a transition at 1.76 MeV followed by positron emission by using a strong source of  $^{90}$ Y in a 40-cm radius of curvature magnetic spectrometer. Very precise measurements of the beta spectrum of  $^{90}$ Y gave no indication of any other group of beta rays between 0.5 MeV and the end point at 2.26 MeV. Further, the authors observed no gamma ray line in the region of 1.76 MeV and they concluded that this energetic transition was to be imputable to that of a monopole between two 0<sup>+</sup> states of the even-even nucleus of  $^{90}$ Zr. They observed an internal conversion line whose intensity relative to that of the 2.26 MeV beta spectrum was  $5 \times 10^{-5}$ . These authors also reported the probability of pair creation per beta decay as:  $w_p / w_p = (2 \pm 1) \times 10^{-4}$ .

One year later Greenberg and Deutsch in a new experiment evaluated the entity of internal pair creation by assessing the number of positron emission relative to the main beta spectrum [4]. They used a magnetic focus arrangement combined with coincidence counting of the annihilation radiation to allow the detection of very low positron intensities in the presence of other radiations. In their paper, the authors noted that in the assessment of the pair production probabilities three types of virtual intermediate states have to be considered. Indicating with  $\psi$  the nuclear wave function one has [4]:

(a) 
$$\psi_{Z} \to \psi_{Z+1} + \beta^{'} + \nu \to \psi_{Z+1} + e^{+} + e^{-} + \beta + \nu$$
  
(b)  $\psi_{Z} \to \psi_{Z}^{'} + e^{+} + e^{-} \to \psi_{Z+1} + e^{+} + e^{-} + \beta + \nu$   
(c)  $\psi_{Z} \to \psi_{Z+1}^{'} + \beta + \nu \to \psi_{Z+1} + e^{+} + e^{-} + \beta + \nu$  (1)

with the prime denoting the virtual intermediate state. They noted that the process (a) and (c) contribute about equally to pair creation, i.e. the pairs are formed by the field of the beta ray and of the residual nucleus.

In order to compare their findings with those obtained by other authors, Greenberg and Deutsch evaluated the internal pair production probability following the theoretical formulation proposed by Thomas [5]. According to this formalism, the E0 transition strength from the initial excited state  $|\psi_{exc}\rangle$  to state  $|\psi_{norm}\rangle$  is defined by:

$$\rho_{exc/norm} = \frac{\left\langle \psi_{norm} \left| \sum_{j} r_{j}^{2} \left| \psi_{exc} \right\rangle \right|}{R^{2}} = \frac{\int \psi_{exc}^{*} \sum_{j} r_{j} \psi_{norm}}{R^{2}} = \frac{M_{E0}}{R^{2}}$$

$$(2)$$

where  $\sum_{i}$  represents a summation over all nuclear protons at positions  $r_i$  and the parameter  $R=1.2A^{1/3}$  fm is the nuclear radius. Therefore the internal pair production probability,  $w_p$ , depends on the relevant matrix  $M_{E0}$  [4-5]. Most notably, they observed that the evaluation of this matrix element could only be estimated from some nuclear models. On the other hand, the *relative* probabilities for the emission of conversion electrons,  $w_K$ , or of a positron electron pair involve only an evaluation of the electron wave functions at the nuclear surface. Using the Thomas formulation for  $w_p$  and  $w_K$  no specific nuclear property, not even the nuclear radius, enter the ratio of internal conversion to internal pair creation.

According to Thomas' formalism the internal pair production probability  $w_p$  is given by the following analytic formula [5]:

$$w_{p} = \frac{32}{9\pi \left[\Gamma(2\gamma + 1)\right]^{4}} M^{2} \alpha^{2} (2R)^{4\gamma - 4} I$$
(3)

where:

$$I = \int_{1}^{E-1} \frac{dx \left[ x(E-x) - \gamma^{2} \right]}{\left\{ \left( x^{2} - 1 \right) \left[ \left( E - x \right)^{2} - 1 \right] \right\}^{\frac{1}{2} - \gamma}} \exp \left\{ \pi \alpha Z \left[ \frac{\left( E - x \right)}{\left[ \left( E - x \right)^{2} - 1 \right]^{\frac{1}{2}}} - \frac{x}{\left[ x^{2} - 1 \right]^{\frac{1}{2}}} \right] \right\}$$

$$\times \left| \Gamma \left( \gamma + i\alpha Z \frac{\left( E - x \right)}{\left[ \left( E - x \right)^{2} - 1 \right]^{\frac{1}{2}}} \right) \right|^{2} \cdot \left| \Gamma \left( \gamma + \frac{i\alpha Zx}{\left[ x^{2} - 1 \right]^{\frac{1}{2}}} \right) \right|^{2}$$

$$(4)$$

with:

 $\gamma = \left[1 - \left(Z\alpha\right)^2\right]^{\frac{1}{2}}$ ,  $\alpha = 1/137$  fine structure constant, R nuclear radius, Z atomic number of the element and  $\Gamma(2\gamma+1)$  denotes the gamma function. In Equation 3, units have been chosen such that  $m, c, \hbar$  are equal to unity.

On the other hand, the probability for the emission of conversion electrons,  $w_K$ , is:

$$w_{K} = \frac{8\left[\left(1-\gamma\right)+3^{\frac{1}{2}}\left(1+\gamma\right)\right]^{2}}{27\left[\Gamma\left(2\gamma+1\right)\right]^{3}}Z^{3}M^{2}\alpha^{5}\left[4Z\alpha PR^{2}\right]^{2\gamma-2}\exp\left\{\pi\alpha Z\frac{W}{P}\right\}\left|\Gamma\left(\gamma+i\alpha Z\frac{W}{P}\right)\right|^{2}$$
(5)

Where  $W = E + \gamma$  is the energy of the outgoing electron, E is the transition energy and P is its momentum of the electron. For large Z (>60), so that  $\{2\pi\alpha Z\}$   $\Box$  1, the following useful approximation may be inserted into Equation (5):

$$\left| \Gamma \left( \gamma + i\alpha Z \frac{W}{P} \right) \right|^2 \to \left[ 3 - 2\gamma \right] 2\pi\alpha Z \frac{W}{P} \exp \left\{ -\pi\alpha Z \frac{W}{P} \right\}$$
 (6)

which also includes the expansion in power of  $(1-\gamma)$ , good for all nuclei with  $Z \le 90$ . Then one immediately obtains the relative probability of the emission of conversion electrons to that of a positron electron pair creation:

$$\frac{w_K}{w_p} = \frac{\Gamma(2\gamma + 1) \left[ (1 - \gamma) + 3^{\frac{1}{2}} (1 + \gamma) \right]^2}{24(3 - 2\gamma)} (Z\alpha)^{2\gamma} P^{2\gamma - 2} \frac{W(W + \gamma)}{I'}$$
(7)

where:

$$I' = \int_{1}^{E-1} \frac{x \left[ x(E-x) \right] \left[ x(E-x) - \gamma^{2} \right]}{\left\{ (x^{2}-1) \left[ (E-x)^{2} - 1 \right] \right\}^{1-\gamma}} \exp \left\{ -\frac{2\pi\alpha Zx}{\left[ x^{2}-1 \right]^{\frac{1}{2}}} \right\} dx$$
 (8)

Following this formalism and resolving Equation (7) for the appropriate energy and atomic number, Greenberg and Deutsch obtained for the ratio of the K-conversion to pair creation:

$$\frac{W_K}{W_p} = 2.6 \tag{9}$$

On the other hand, one year before, Johnson and colleagues reported an internal conversion intensity relative to that beta spectrum  $w_K/w_\beta=5\times10^{-5}$  and a probability of pair creation per beta decay  $w_p/w_\beta=(2\pm1)\times10^{-4}$ . As a consequence, using the experimental data obtained by Johnson, one would obtain:

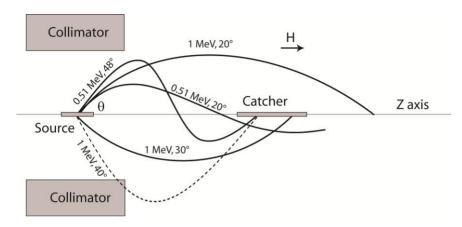
$$\frac{w_K}{w_p} = 0.25 \tag{10}$$

uncertain to about a factor of two. In view of this substantial discrepancy of the  $w_K/w_p$  ratio obtained by the two authors, Greenberg and Deutsch decided to measure the number of positrons per beta decay of  $^{90}$ Y with their apparatus.

The experimental problem Greenberg and Deutsch had to face consisted of the detection of a very small number of primary positrons in the presence of an overwhelmingly larger number of other radiations (beta rays, internal/external bremsstrahlung radiations and secondary positrons produced by the impact of photons and beta rays). The low relative intensity of the effect sought, made it imperative to use a very selective detection method. Such a method was allowed by the annihilation radiation produced when the positrons were stopped in a beryllium target (referred to as the "catcher"). The two annihilation gammas arising in the target were detected coincidently using two sodium iodide (NaI) detectors. To minimize the formation of positrons by energetic electrons or photons striking the catcher, the latter was located in a magnetic field in such a position that about one-half of all the positrons emitted by the source in the interesting energy interval would strike it while all trajectories of

electrons with energy greater than 1 MeV either missed the catcher or were intercepted by the collimator (Figure 2).

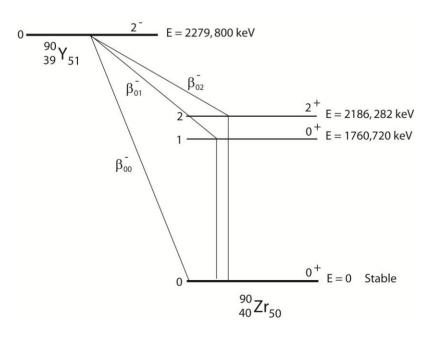
**Figure 2.** Experimental apparatus used by Greenberg and Deutsch for the detection of positrons emitted from a <sup>90</sup>Y source due to 1.75 MeV electric monopole transition to <sup>90</sup>Zr. Image reproduced from reference [4].



From their experiment, the positron branch ratio was determined to be  $w_p / w_\beta = (3.6 \pm 0.9) \times 10^{-5}$ . Combined with the data for the intensity of the conversion line obtained by from Johnson and colleagues, they obtained an experimental value for the probability of pair creation per beta decay as  $w_K / w_p = 1.4$ , in moderate agreement with the calculation of Thomas.

Later on, in 1961, in an attempt to quantify a predicted two gamma emission in the 0+/0+ transition of  $^{90}$ Zr by Ryde *et al*. [6], Langhoff and Hennies [7] determined with a scintillation coincidence spectrometer the positron branch ratio to be  $w_p / w_\beta = (3.4 \pm 0.4) \times 10^{-5}$  and a relative probability of the emission of conversion electrons to that of total beta decays to be  $w_K / w_\beta = (8.1 \pm 1.1) \times 10^{-5}$ .

Figure 3. Decay scheme of <sup>90</sup>Y



In recent years, Selwyn and colleagues [8] used a high-purity germanium detector to determine the internal pair production branch ratio of the  $0^+$  –  $0^+$  transition of  $^{90}$ Zr. The basic measurement technique consisted in counting the gross number of gammas detected within a 511 keV (annihilation) peak and subtracting the bremsstrahlung continuum, environmental continuum, and environmental peak at 511 keV. The germanium detector was selected over other detectors (i.e., NaI and CdTe) based on its superior energy resolution. In the measurement, it is fundamental to quantify the extremely small 511 keV peak observed above the large bremsstrahlung spectrum and environmental 511 keV background. The authors found the branch ratio to be  $w_p/w_\beta = (3.186 \pm 0.047) \times 10^{-5}$ . Figure 3 shows the decay scheme of  $^{90}$ Y, while in Table 1 the experimental values for the internal pair production branch ratio of the  $0^+/0^+$  transition of  $^{90}$ Zr are reported.

**Table 1.** Probability of pair creation per beta decay measured in earlier and more recent literature studies.

Reference	$w_p / w_\beta$	Detector
Johnson <i>et al.</i> (1955)	$(2\pm1)\times10^{-4}$	NaI
Greenberg and Deutsch (1955)	$(3.6\pm0.9)\times10^{-5}$	NaI
Langhoff and Hennies (1961)	$(3.4\pm0.4)\times10^{-5}$	NaI
Selwyn <i>et al.</i> (2006)	$(3.186\pm0.047)\times10^{-5}$	HPGe

Tables 2 and 3 report the most updated properties of <sup>90</sup>Y beta decay, from LNHB/CEA [9].

**Table 2.** Beta minus transitions of <sup>90</sup>Y

	Energy (keV)	Probability (x 100)	Nature
$\beta_{02}^{\scriptscriptstyle -}$	93.5 (17)	0.0000014 (3)	1 <sup>st</sup> forbidden
$oldsymbol{eta}_{01}^-$	519,1 (17)	0,017 (6)	Unique first forbidden
$oldsymbol{eta_{00}^-}$	2279,8 (17)	99,983 (6)	Unique first forbidden

**Table 3.** Gamma transitions of <sup>90</sup>Y, including conversion electron (ce)

	Energy (keV)	Probability γ+ce (x 100)	Multipolarity
$\gamma_{10}(Zr)$	1760,7 (2)	0.0000014 (3)	E0
$\gamma_{20}(Zr)$	2186,282 (10)	0,017 (6)	E2

# 3. Exploitation in Nuclear Medicine of the $\beta^+/\beta^-$ Emission from the $0^+-0^+$ Transition of $^{90}Zr$

 $^{90}\mathrm{Y}$  is one of the most widely used radionuclide for internal radiotherapy as the long range of the  $\beta$  particles allows more uniform irradiation in large tumours [10]. Therefore,  $^{90}\mathrm{Y}$  labelling is currently adopted for preparation of compounds belonging to various classes of therapeutic agents: peptides, antibodies, microspheres and citrate. In addition,  $^{90}\mathrm{Y}$  is also used to label resin or glass microspheres for liver radioembolization, an interventional radiology procedure in which millions of  $^{90}\mathrm{Y}$  microspheres are infused through a catheter into the hepatic artery. According to this procedure, the

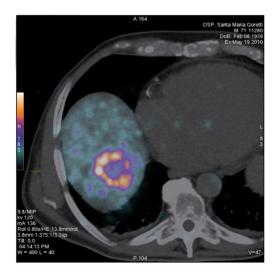
microspheres become embedded in the liver, and the therapeutic dose is delivered over a period of about two weeks allowing <sup>90</sup>Y to irradiate the tumor while sparing healthy liver tissue.

Different authors have used the small positronic emission of <sup>90</sup>Y to obtain high-resolution positron emission tomography (PET) images of <sup>90</sup>Y-labelled radiopharmaceuticals. In 2004, Nickles *et al.* assessed <sup>90</sup>Y distribution on a Derenzo phantom using a micro-PET scanner provided with bismuth germanate (BGO) crystals showing the remarkable resolution and quantitative accuracy of positron tomography [11]. In the same paper they concluded that <sup>90</sup>Y provide a "clear picture of the regional dose delivered by the therapy".

However, the issue associated with  $^{90}Y$  PET imaging is the extremely small emission probability of the  $\beta^+$  particles. In order to visualize (and properly measure) the activity taken up by a region of interest, a high  $^{90}Y$  concentration is required. In liver radioembolization the typically injected activity ranges from one to several GBq and the total amount of radioactivity is concentrated in the liver or in small regions inside it. Hence high  $^{90}Y$  concentration regions may be obtained with this technique and PET imaging of  $^{90}Y$  is possible.

Recently, accurate biodistribution assessment after microsphere administration by direct  $^{90}$ Y-PET scan after liver radioembolization was proven feasible by Lhommel *et al.* [12-13] and Werner *et al.* [14] which used a TOF-PET equipped with lutetium-yttrium-oxyorthosilicate (LYSO) crystals and a non-TOF PET/CT with lutetium oxyorthosilicate (LSO) detectors, respectively. The results obtained by these authors pioneered further studies about the possibility of detecting the  $\beta^+$  particles emitted by  $^{90}$ Y during internal radiotherapy treatments. In another work, Gates *et al.* [15] showed the feasibility of hepatic localization of microsphere using routine PET on three patients concluding that  $^{90}$ Y microspheres can be visualized with a simple 20-min PET/CT scan acquired using universally available technology. Bagni *et al.* confirmed the feasibility of  $^{90}$ Y PET imaging for the assessment of microsphere biodistribution (Figure 4) using a routine PET/CT scanner provided with BGO crystals [16]. Recent studies performed by D'Arienzo *et al.* [17] and Willowson *et al.* [18] confirmed the feasibility of dosimetry and quantitative image reconstruction following  $^{90}$ Y PET, respectively.

**Figure 4.** PET acquisition of  $\beta^+$  particles emitted in the  $0^+/0^+$  transition of  $^{90}$ Zr. The biodistribution of resin microspheres after liver radioembolization is shown (courtesy of Dr. Oreste Bagni).



Finally, it is worth mentioning that another study by Fabbri *et al.* [18] considered clinical applications of <sup>90</sup>Y PET scans in locoregional therapies other than liver radioembolization.

### 4. Conclusions

Precise knowledge of the branch ratio of the  $0^+$   $0^+$  transition of  $^{90}$ Zr is important for an accurate quantification of  $^{90}$ Y accumulated inside the target region and detected via PET acquisition. Most recent literature findings report an internal pair production branch ratio as large as  $(3.186\pm0.047)\times10^{-5}$ , measured by Selwyn and colleagues using a HPGe detector. Different studies indicate that the high-resolution images attainable with  $^{90}$ Y PET may allow for accurate patient dosimetry after locoregional administration of  $^{90}$ Y for therapeutic purposes.

## **References and Notes**

- 1. Schirmer, J.; Habs, D.; Kroth, R. Double Gamma Decay in <sup>40</sup>Ca and <sup>90</sup>Zr. *Phys. Rev.* **1984**, *53*, 1897.
- 2. Ford, K. Predicted 0<sup>+</sup> level of Zr<sup>90</sup>. *Phys. Rev.* **1955**, 98, 1516.
- 3. Johnson, O.; Johnson, R.; Langer, L. Evidence for a 0+ first excited state in Zr<sup>90</sup>. *Phys. Rev.* **1955**, 98, 1517–1518.
- 4. Greenberg, J.S.; Deutsch, M. Positrons from the decay of P<sup>32</sup> and Y<sup>90</sup>. *Phys. Rev.* **1956**, *102*, 415–421.
- 5. Thomas, R. Internal pair production in radium C'. Phys. Rev. 1940, 58, 714–715.
- 6. Ryde, H.; Thieberger, P.; Alvager, T. Two-photon de-excitation of the 0<sup>+</sup> level in Zr<sup>90</sup>. *Phys. Rev. Lett.* **1961**, *6*, 475–476.
- 7. Langhoff, H.; Hennies, H. Zum experimentellen Nachweis von Zweiquantenzerfall beim 0<sup>+</sup>–0<sup>+</sup> Ubergang des Zr<sup>90</sup>. *Zeitschrift fur Physik* **1961**,*164*, 166–173.
- 8. Selwyn, R.G.; Nickles, R.J.; Thomadsen, B.R.; DeWerd, L.A.; Micka, J.A. A new internal pair production branching ratio of 90Y: the development of a non-destructive assay for <sup>90</sup>Y and <sup>90</sup>Sr. *Appl. Radiat. Isot.* **2006**, *65*, 318-327.
- 9. Bé, M.-M.; Chisté, V.; Dulieu, C.; Mougeot, X.; Browne, E.; Chechev, V.; Kuzmenko, N.; Kondev, F.; Luca, A.; Galán, M.; Arinc, A.; Huang, X. Table of Radionuclides, Monographie BIPM-5, **2010**, ISBN 92-822-2207-7.
- 10. Brans, B.; Linden, O.; Giammarile, F.; Tennvall, J.; Punt, C. Clinical applications of newer radionuclide therapies. *Eur. J. Cancer* **2006**, *42*, 994–1003.
- 11. Nickles, R.J.; Roberts, A.D.; Nye, J.A.; Converse, A.K.; Barnhart, T.E.; Avila-Rodirguez, M.A. Assaying and PET imaging of yttrium-90: l>>34 ppm>0. *IEEE Nuclear Science Symposium Record* **2004**, *6*, 3412-3414.
- 12. Lhommel, R.; Goffette, P.; Van den Eynde, M.; Jamar, F.; Pauwels, S.; Bilbao, J.; Walrand, S. Yttrium-90 TOF PET scan demonstrates high-resolution biodistribution after liver SIRT. *Eur. J. Nucl. Med. Mol. Imaging* **2009**, *36*, 1696.
- 13. Lhommel, R.; van Elmbt, L.; Goffette, P.; Van den Eynde, M.; Jamar, F.; Pauwels, S.; Walrand, S. Feasibility of <sup>90</sup>Y TOF PET-based dosimetry in liver metastasis therapy using SIR-Spheres. *Eur. J. Nucl. Med. Mol. Imaging* **2010**, *37*, 1654–1662

14. Werner, M.K.; Brechtel, K.; Beyer, T.; Dittmann, H.; Pfannenberg, C.; Kupfershlager, J. PET/CT for the assessment and quantification of <sup>90</sup>Y biodistribution after selective internal radiotherapy (SIRT) of liver metastases. *Eur. J. Nucl. Med. Mol. Imaging* **2010**, *37*, 407–408.

- 15. Gates, V.L.; Esmail, A.A.; Marshall, K.; Spies, S.; Salem, R. Internal pair production of 90Y permits hepatic localization of microspheres using routine PET: proof of concept. *J. Nucl. Med.* **2011**, *52*, 72–76.
- 16. Bagni, O.; D'Arienzo, M.; Chiaramida, P.; Chiacchiararelli, L.; Cannas, P.; D'Agostini, A.; Cianni, R.; Salvatori, R.; Scopinaro, F. <sup>90</sup>Y-PET for the assessment of microsphere biodistribution after selective internal radiotherapy (SIRT). *Nucl. Med. Commun.* **2012**, *33*, 198–204.
- 17. D'Arienzo, M.; Chiaramida, P.; Chiacchiararelli, L.; Coniglio, A.; Cianni, R.; Salvatori, R.; Ruzza, A.; Scopinaro, F.; Bagni, O. 90Y PET-based dosimetry after selective internal radiotherapy treatments. *Nucl. Med. Commun.* **2012**, *33*, 633–640
- 18. Willowson, K.; Forwood, N.; Jakoby, B.W.; Smith, A.M.; Bailey, D.L. Quantitative <sup>90</sup>Y image reconstruction in PET. *Med. Phys.* **2012**, *39*, 7153–7159.
- 19. Fabbri, C.; Mattone, V.; Casi, M.; De Lauro, F.; Agostini, M.; Bartolini, N.; D'Arienzo, M.; Marchi, G.; Bartolomei, M.; Sarti, G. Quantitative Evaluation On <sup>90</sup>Y-DOTATOC PET And SPECT Imaging By Phantom Acquisitions And Clinical Applications In Locoregional And Systemic Treatments. *Q. J. Nucl. Med. Mol. Imaging* **2012**, *56*, 522–528.
- © 2013 by the authors; licensee MDPI, Basel, Switzerland. This article is an open access article distributed under the terms and conditions of the Creative Commons Attribution license (http://creativecommons.org/licenses/by/3.0/).